MICHAŁ PAZDANOWSKI*

RESIDUAL STRESSES AS A FACTOR OF RAILROAD RAIL FATIGUE

NAPRĘŻENIA RESZTKOWE JAKO CZYNNIK ZMĘCZENIA SZYN KOLEJOWYCH

Abstract

An analysis of the influence of residual stresses on material fatigue is presented in this paper. Residual stress distribution in railroad rails subjected to simulated service loads is considered. A mechanical model based on the plastic shakedown theory was used to determine residual stresses and the Dang Van fatigue criterion was applied.

Keywords: *residual stresses*, *material fatigue*, *Dang Van criterion*

Streszczenie

W artykule przedstawiono analizę wpływu naprężeń resztkowych wywołanych symulowanym obciążeniem szyn kolejowych kołami taboru kolejowego na zmęczenie materiału szyny. Do wyznaczenia rozkładu naprężeń resztkowych zastosowano model mechaniczny oparty na teorii plastycznego przystosowania, a jako kryterium zmęczeniowe przyjęto kryterium Dang Vana.

Słowa kluczowe: *naprężenia resztkowe*, *zmęczenie materiału*, *kryterium Dang Vana*

* Ph.D. Michał Pazdanowski, Institute for Computational Civil Engineering, Faculty of Civil Engineering, Cracow University of Technology.

1. Introduction

Railroad rails may catastrophically fail during service resulting in loss of human life and significant damage to rolling stock [1, 2]. The experimental investigations [3] revealed that residual stresses induced in a rail during manufacturing (roller straightening) and service (contact loads at the rail/wheel interface, exceeding the elastic bearing capacity of the rail material) may constitute an important factor affecting crack nucleation and growth.

In the current paper, the influence of residual stresses induced in a railroad rail during simulated service on the fatigue life of such a rail is given consideration.
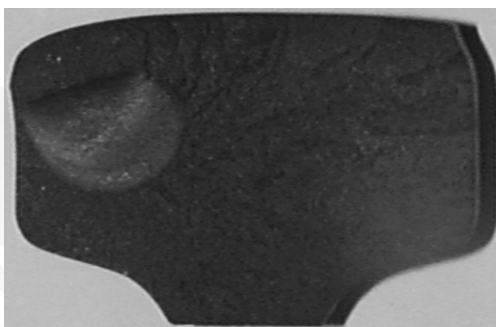
Fig. 1. Initiation and growth of fatigue crack in the head of rail subjected to service loads

Residual stresses in rails subjected to service conditions may be found through either numerical analysis [21], or through experimental investigations of specimens taken out of standard revenue tracks [22] or test tracks [23]. Experimental analysis is time consuming, costly and in the case of specimens taken out of revenue tracks, the loading history of a specimen may be impossible to ascertain. On the other hand, numerical analysis may be prohibitively time consuming when an exact elasto-plastic incremental analysis would have to be performed in order to find the final residual stress state in a rail after a significant number of loading cycles [21]. This obstacle may be avoided when one settles for an estimate of residual stress distribution in a rail subjected to *simulated* service loads computed using the mechanical model based on the elasto-plastic shakedown theorem initially proposed in [4, 5]. Although the application of this mechanical model yields only an estimate of residual stresses induced by simulated service loads, numerous tests have shown that this estimate is of reasonably good quality [6].

Multiaxial high cycle fatigue criteria for metals may be divided into three main groups [7]: critical plane approaches, such as Findley [10], Matake [11], McDiarmid [12], Dietmann [13]; approaches based on stress invariants, such as Marin [14], Crossland [15], Kakuno-Kawada [16], Deperrois [17]; approaches based on stress averages within the elementary volume, such as Grubisic and Simburger [18], Liu and Zenner [19], or Dang Van [20]. According to [7], criteria belonging to the group of approaches based on the stress averages within material volume yield results closest to experiments for so called 'hard' metals (which include steels). Therefore, the simplest of these, the Dang Van [20] criterion, was used in further analysis.

2. Residual stress evaluation method

The residual stress calculation method based on shakedown theorems [9], in its simplest form may be stated as the following minimization problem [5]:
find:

$$\min_{\sigma_{ij}^r} \int_V (\sigma_{kl}^r - \sigma_{kl}^0)^T \cdot C_{ijkl} \cdot (\sigma_{ij}^r - \sigma_{ij}^0) \cdot dV \qquad (1)$$

subject to:

$$\sigma_{ij,j}^r = 0 \quad - \text{ for each point in } V \qquad (2.1)$$

$$\sigma_{ij}^r \cdot n_j = 0 \quad - \text{ for each point on } \delta V \qquad (2.2)$$

$$\Phi(\sigma_{ij}^r + \sigma_{ij}^E(t)) \leq \sigma_y \quad - \text{ for each point in } V \qquad (2.3)$$

where:

$\sigma_{ij}^r, \sigma_{kl}^r$ – time independent residual stresses induced in the considered body by the actual loading program,

$\sigma_{ij}^0, \sigma_{kl}^0$ – initial residual stresses existing in the considered body prior to the application of current loading program,

σ_{ij}^E – time dependent elastic stresses induced in the body by current loading program changing in time,

s_y – material yield limit,

C_{ijkl} – elastic compliance matrix,

n_j – vector perpendicular to the body boundary.

Formula (1) denotes the total complementary energy of residual stresses while formulas (2.1) and (2.2) denote the internal equilibrium conditions and zero static boundary conditions of those stresses. Formula (2.3) denotes the yield condition, which has to be satisfied in every moment of time. Of course, all the constraints (2) have to be satisfied in every point of the considered body.

3. The Dang Van fatigue criterion

The Dang Van fatigue criterion may be counted among the fatigue criteria based on the mesoscopic scale approach, i.e. the scale of metal grains of a metallic aggregate [7]. Thisfatigue criterion is based on an average measure of the plastic strain accumulated in all the flowing crystals within an elementary volume of the material.

This criterion condenses the history of six stress tensor components into the load path defined by two components, and thus simplifies fatigue damage calculations [8]. The criterion combines hydrostatic pressure σ_H and momentary maximum shearing stress τ_a calculated according to the Tresca criterion:

$$\tau_a(t) = \frac{1}{2} \cdot \left[s_I^v(t) - s_{III}^v(t) \right] \tag{3}$$

evaluated for the part of stress deviator tensor which varies in time; this part is defined as:

$$s_{ij}^v(t) = s_{ij}(t) - s_{ij}^c = [\sigma_{ij}(t) - \delta_{ij} \cdot \sigma_H(t)] - s_{ij}^c \tag{4}$$

where s_{ij}^c constitutes the solution of the following minimax problem:

$$s_{ij}^c = \min_{s_{ij}^*} \max_t (s_{ij}(t) - s_{ij}^*) \cdot (s_{ij}(t) - s_{ij}^*) \tag{5}$$

i.e. such value of the time independent stress deviator s_{ij}^* for which the maximum of the norm (5) reaches the lowest value. Shear stress and hydrostatic pressure are then combined linearly to yield an equivalent scalar:

$$\tau_{eq,DV} = \max_t (\tau_a(t) + \alpha \cdot \sigma_H(t)) \tag{6}$$

which in turn may be used to estimate the fatigue damage [8].

The constant α is determined as follows:

$$\alpha = 3 \cdot \left(\frac{\tau_D}{\sigma_D} - \frac{1}{2} \right) \tag{7}$$

where τ_D and σ_D represent fatigue limits in torsion and tension-compression, respectively. According to the Dang Van criterion, time independent residual stresses do not affect the momentary maximum shear stress τ_a (3), but affect only the hydrostatic stress term σ_H [8].

4. Service load simulation program

The contact load acting on the rail crown has been simulated by biparabolic pressure distribution spanned over the rectangular contact area applied at seven evenly distributed discrete contact locations shown in Fig. 2, where location 1 is centered on the rail's longitudinal axis of symmetry while location 7 is offset by 25 mm to the left of this axis. Peak pressure p_0 and patch dimensions $a \times b$ have been determined using elastic Hertz contact formulae to compute the contact ellipse area for the given contact load, and later on, to determine a rectangle with equivalent area and biparabolic pressure distribution balancing this contact load. For the purpose of current calculations, 132RE rail (US type) made of steel exhibiting the following material data have been assumed: 206 GPa Young Modulus, 483 MPa yield limit, 0.3 Poisson's ratio. Three values of wheel load have been considered, namely: 147 kN, 160 kN, 173 kN. These values correspond to standard wheel loads on heavy haul rail lines in North American practice.

A 3D Finite Element Method computational model was used to find the necessary momentary elastic stress distributions σ_{ij}^E (2.3), while a 2D Meshless Finite Difference Method computational model was applied to determine the rail longitudinal axis independent distributions of residual stresses σ_{ij}^r.
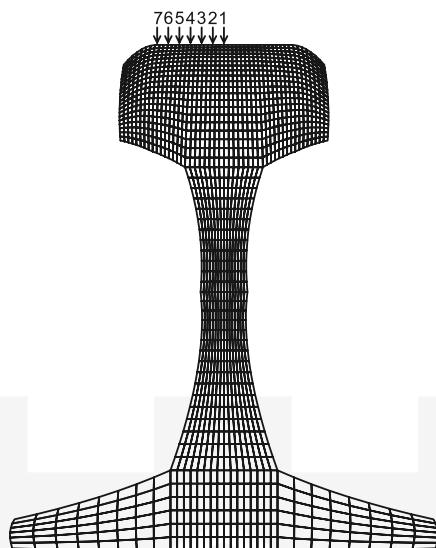
Fig. 2. Load application points on the rail crown and mesh used during numerical analysis

Peak residual and elastic hydrostatic stress levels introduced in rail

Location (Fig. 2)	Load [kN]	Compression [MPa]		Tension [MPa]	
		residual σ_H^r	elastic σ_H^r	residual σ_H^r	elastic σ_H^r
2		−107.900	−496.460	78.733	−197.260
4	147	−130.622	−438.299	80.716	−197.779
6		−140.146	−432.423	97.209	−188.910
2		−120.254	−407.357	79.491	−209.653
4	160	−126.147	−423.772	81.502	−211.301
6		−140.023	−459.753	108.147	−192.702
2		−142.589	−446.350	107.429	−187.212
4	173	−147.962	−371.866	116.255	−187.289
6		−171.047	−369.222	153.002	−165.418

The distribution of hydrostatic residual stress σ_H^r (directly affecting the Dang Van fatigue criterion) in the railhead for all three considered values of wheel load applied at the rightmost load application point depicted in Fig. 2 is presented in Fig. 3. For better readability, tensile and compressive parts of this stress are depicted separately on the right and left, respectively. Peak residual hydrostatic pressure levels introduced by each of the considered

loading scenarios at selected loading locations are presented in Table 1. and compared to the highest elastic (momentary) hydrostatic pressure levels introduced by simulated wheel load introduced at the same locations in the railhead.
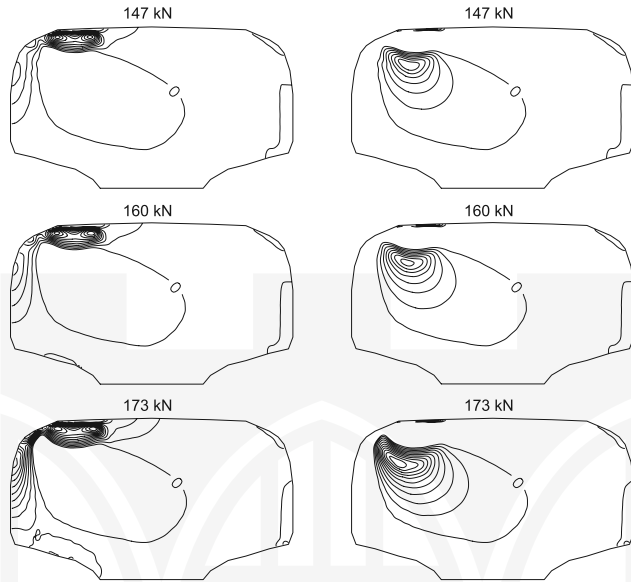
Fig. 3. Hydrostatic residual stress σ_H^r decomposed into positive (compression – at left) and negative (tension – at right) parts. Contour interval 14 MPa

Locations of peak hydrostatic residual stresses σ_H^r (compressive component denoted by ○, and tensile component denoted by ●) as well as von Mises equivalent residual stresses σ_0^r (denoted by □) corresponding to load application points indicated in Fig. 2 are depicted in Fig. 4.
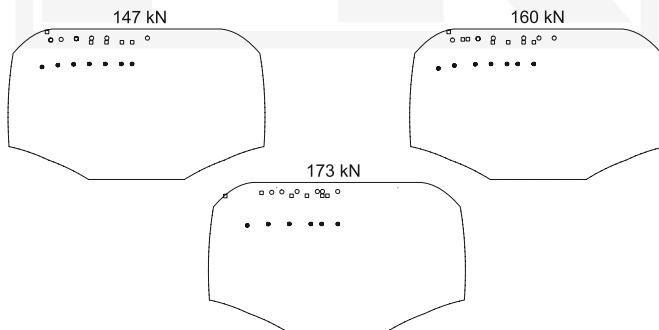
Fig. 4. Location of extreme values of hydrostatic residual stress and von Mises equivalent residual stress induced by contact loads applied at locations indicated in Fig. 2

5. Conclusions

Initial calculations performed so far indicate that the residual stress levels due to simulated contact loads may reach levels on a par with actual (momentary) elastic stresses created by these loads, and thus should be included in fatigue calculations. Values of these stresses tend to increase substantially (by up to 23.5% in compression and up to 30.1% in tension for the results presented in Table 1) as the load application area shifts away from the center of the railhead. When the load application area gets very close to the gauge side of the rail an additional stress concentration zone occurs at the gauge side of railhead. This phenomenon may additionally be aggravated should two point contact load occur (for instance on a curved track). Thus, two point contact loads will be subjected to analysis in further work.

The results presented in the 5th column of Table 1 are of special interest from the practical point of view, as the tensile stresses have an adverse influence on the fatigue life of the body subject to cyclic loads. The residual hydrostatic tension for loading scenarios considered so far reaches a level of almost 32% of the material yield limit, thus indicating that these stresses significantly affect rail fatigue life, and the safety of railroad operation.

The location of extreme residual hydrostatic stresses below the running surface of the rail remains fairly stable, regardless of the load application point location, though the depth of extreme stresses seems to be affected by the load magnitude for tensile stresses only.

At the locations indicated in Fig. 4 by ●, the residual hydrostatic pressure for higher wheel loads is on par with the elastic hydrostatic pressure. The positive sign of this pressure (tension) indicates substantially increased risk of rail failure fatigue in this zone.

References

[1] Steel R.K., et al, *Catastrophic web cracking of railroad rail: A discussion of the unanswered questions*, AAR, 1990.

[2] Zerbst U., Lunden R., Edel K.-O., Smith R.A., *Introduction to the damage tolerance behaviour of railway rails – a review*, Engineering Fracture Mechanics, vol. 76, 2009, 2563-2601.

[3] Groom J.J., *Determination of residual stresses in rails*, Batelle Columbus Laboratories, Rpt. No. DOT/FRA/ORD 83-05 Columbus OH, 1983.

[4] Orkisz J., Harris A., *Analysis of residual stresses at shakedown, a hybrid approach*, Theoretical and Applied Fracture Mechanics, vol. 9, 1988, 109-121.

[5] Orkisz J., et al., *Discrete analysis of actual residual stresses resulting from cyclic loadings*, Computers and Structures, vol. 35, 1990, 397-412.

[6] Pazdanowski M., *On estimation of residual stresses in rails using shake-down based method*, Archives of Transport, vol. 22(3), 2010, 319-336.

[7] Papadopulos I.V., Davoli P., Gorla C., Filippini M., Bernasconi A., *A comparative study of multiaxial high-cycle fatigue criteria for metals*, International Journal of Fatigue, vol. 19(3), 1997, 219-235.

[8] Bernasconi A., Davoli P., Filippini M., Foletti S., *An integrated approach to rolling contact sub-surface fatigue assessment of railway wheels*, Wear, vol. 258, 2005, 973-980.

[9] Martin J.B., *Plasticity – fundamentals and general results*, The MIT Press, 1975.

[10] Findley W.N., *A theory for the effects of mean stress on fatigue of metals under combined torsion and axial load or bending*, Journal of Engineering for Industry, vol. 11, 1959, 301-306.

[11] Matake T., *An explanation on fatigue limit under combined stress*, Bull JSME, vol. 20(141), 1977, 257-263.

[12] McDiarmid D.L., *A general criterion for high cycle multiaxial fatigue failure*, Fatigue and Fracture of Engineering Materials and Structures, vol. 14, 1990, 429-453.

[13] Dietmann H., Bhonghibhat T., Schmid A., *Multiaxial fatigue behaviour of steels under in-phase and out-of-phase loading, including different waveforms and frequencies* [in:] D. Kussmaul, D.L. McDiarmid, D. Socie (Eds.): *Fatigue under biaxial and multiaxial loading*, MEP, London 1991, 449-464.

[14] Marin J., *Mechanical behavior of engineering materials*, Prentice-Hall, Englewood Cliffs, N.J., 1962.

[15] Crossland B., *Effect of large hydrostatic pressure on the torsional fatigue strength of an alloy steel* [in:] *Proceedings of the international conference on fatigue of metals*, IME London 1956, 138-149.

[16] Kakuno H., Kawada Y., *A new criterion of fatigue strength of a round bar subjected to combined static and repeated bending and torsion*, Fatigue and Fracture of Engineering Materials and Structures, vol. 2, 1979, 229-236.

[17] Deperrois A., *Sur le calcul de limites d'endurance des aciers*, PhD thesis, Paris 1995.

[18] Grubisic V., Simburger A., *Fatigue under combined out-of-phase multiaxial stresses* [in:] *Fatigue, Testing and Design*, Proc. SEE Conf., vol. 2, London 1976, 1-28.

[19] Zenner H., SimburgerA., Liu Z., *On the fatigue limit of ductile metals under complex multiaxial loading*, International Journal of Fatigue, vol. 22, 2000, 137-145.

[20] Dang Van K., Griveau B., Message O., *On new multiaxial fatigue criterion: theory and application* [in:] *Biaxial and multiaxial fatigue*, MEP, London 1989, 479-496.

[21] Ringsberg J.W., Lindback T., *Rolling contact fatigue of rails including numerical simulations of the rail manufacturing process and repeated wheel rail contact loads*, International Journal of Fatigue, vol. 25, 2003, 547-558.

[22] Groom J.J., *Determination of residual stresses in rails*, Batelle Columbus Laboratories, Rpt. DOT/FRA/ORD-83-05, Columbus, OH, 1983.

[23] Lo K.H., Mummery P., Buttle D.J., *Characterization of residual principal stresses and their implications on failure of railway rails*, Engineering Failure Analysis, vol. 17, 2010, 1273-1284.